Sparse Channel Estimation for DCO-OFDM VLC Systems in the Presence of Clipping Noise

Ekin Basak Bektas (ekin.bektas@khas.edu.tr)
Kadir Has University https://orcid.org/0000-0001-8826-5756
Erdal Panayirci
Kadir Has Universitesi - Cibali Merkez Kampusu: Kadir Has Universitesi

Research Article

Keywords: Visible light communications, VLC, Nonlinear clipping noise, Channel estimation, DC biased optical OFDM (DCO-OFDM)

Posted Date: June 4th, 2021

DOI: https://doi.org/10.21203/rs.3.rs-380210/v1

Noname manuscript No.
(will be inserted by the editor)

Sparse Channel Estimation for DCO-OFDM VLC Systems in the Presence of Clipping Noise

Ekin Basak Bektas · Erdal Panayirci

Received: date / Accepted: date

Abstract —In this paper, a new iterative channel estimation algorithm is proposed that exploits channel sparsity in the time domain for DC-biased optical orthogonal frequency division multiplexing OFDM (DCO-OFDM) systems in indoor visible light communications (VLC) in the presence of a clipping noise. A path-based channel model is used, in which the channel is described by a limited number of paths, each characterized by a delay and channel gain. Making use of the pilot symbols, overall sparse channel tap delays and path gains were initially estimated by the compressed sensing approach, in the form of the Orthogonal Matching Pursuit (OMP) and the least-squares (LS) algorithms, respectively. Then a computationally efficient and novel iterative channel estimation algorithm is developed that estimates the clipping noise in the time-domain and compensated for its effect in the frequency-domain. Computer simulation results show that the algorithm converges in maximum two iterations and that yields excellent mean square error (MSE) and bit error rate (BER) performance, outperforming those channel estimation algorithms, which do not have the clipping noise mitigation capability.

Keywords Visible light communications · VLC · Nonlinear clipping noise · Channel estimation · DC biased optical OFDM (DCO-OFDM)

Ekin Basak Bektas
Department of Electrical-Electronics Engineering, Kadir Has University, Cibali-Fatih, 34083 Istanbul, Turkey
E-mail: ekin.bektas@khas.edu.tr

Erdal Panayirci
Department of Electrical-Electronics Engineering, Kadir Has University, Cibali-Fatih, 34083 Istanbul, Turkey
E-mail: eepanay@khas.edu.tr

1 Introduction

Limited radio frequency spectrum imposes restrictions on the increase in the ubiquitous and high capacity connection demand in wireless communication. As the upper limit of the RF band is approaching, alternative telecommunication systems to RF technology are being developed, especially for the 6th generation and beyond mobile systems. Herein, optical wireless communication (OWC) technology is emerging as a promising complementary technology for RF communications. Visible light communication (VLC) systems, which are part of OWC, solve the problem of low bandwidth in RF communication by occupying the 380 nm to 750 nm spectrum corresponding to the 430 THz to 790 THz frequency spectrum [1]. Additively, VLC has an unregulated spectrum and is immune to security issues arising in RF communication systems. It can be used in RF restricted areas such as aircraft, library, hospital, etc., and also used for illumination.

On the other hand, orthogonal frequency division multiplexing (OFDM) is increasingly recognized as a physical transmission technique for OWC [2], as it has better optical power efficiency compared to conventional modulation schemes. In conventional OFDM, the transmitted signals are bipolar and complex. However, since the light intensity could not be negative, bipolar signals cannot be transmitted in an intensity-modulated / direct detection (IM/DD) optical wireless system. Therefore, OFDM signals designed for IM / DD systems must be real and positive. Direct-current biased OFDM (DCO-OFDM) is one of the forms of OFDM used for IM / DD systems in which a DC bias is added to the signal to make the signal positive and all subcarriers carry data symbols [3]. For the DCO-OFDM receiver to operate at an acceptable bit error rate (BER) performance, the channel estimation and equalization processes must be performed perfectly on the receiver side. Due to the constraint that the signals transmitted through the optical channel in VLC systems are only real-valued and positive, the signals reaching the receiver will inevitably be affected by clipping noise and additive Gaussian noise [4]. Furthermore, since the electrical supply of the LEDs connected in series with a cable causes a certain time delay, the impulse response of the optical channel between the transmitter and receiver of the system occurs sparsely and in a frequency selective structure. Therefore, the channel estimation algorithm to be used in the receiver needs to be designed considering the sparse channel model and clipping noise. Up to the present, there has not been much work in the literature on optical sparse channel estimation under clipping noise for VLC systems. In [5,6], several pilot-based channel estimation algorithms have been proposed for DCO-OFDM systems, assuming clipping noise is zero-mean Gaussian noise in addition to the usual additional white Gaussian noise distorting the system. In [7], a superimposed training approach is proposed for channel estimation in DCO-OFDM VLC scenarios. Looking at the channel estimation studies carried out in recent years in visible light communications, the following studies stand out. In [8–10], compressive sensing channel estimation models techniques are proposed for MIMO-OFDM VLC systems. Another

channel estimation algorithm for optical OFDM is presented in [11]. In this work, a least squared-based channel estimation algorithm is proposed for multiuser MISO-VLC. In [12] Adaptive Statistical Bayesian minimum mean square error channel estimation is presented for indoor downlink VLC system. In [13], a channel estimation scheme based on Deep Neural Networks (DNN) for VLC system is proposed. According to the research results, the proposed estimation scheme performs as well as conventional channel estimation schemes.

The main contributions of this paper can be summarized as follows. (i) A special type of the VLC channels is considered for modeling the the optical channels whose impulse responses occur in a sparse and frequency-selective structure, as the electrical supply of the LEDs connected in series with a cable causes certain time delays. (ii) A new channel estimation algorithm with fast and iterative structure is proposed for VLC channel estimation, where the clipping noise is estimated in the time- domain and compensated for its effect in the frequency-domain. (iii) The initial values of the channel, including sparse channel path delays and path gains are determined by the Least-Squares (LS) and the orthogonal matching pursuit (OMP) algorithms, respectively, by means of the pilots symbols. Hence, the computational complexity of the algorithm is greatly reduced by the estimation of very few channel parameters.

The remainder of the paper is organized as follows. Section 2 presents the system model for an OFDM-based VLC system and describes the main parameters of the channel and the clipping noise. Section 3 proposes a new sparse channel estimation algorithm that is based on reducing the efect of the clipping noise in an iterative way. Section 4 provides computer simulations for investigation of mean-squared error (MSE) and bit error performances of the DCO-biased OFDM systems.

2 System Model

In this work, our system model is assumed to be a DCO-OFDM VLC system with N subcarriers. In DCO-OFDM systems, a DC bias is added to make the signal positive, making the data symbols of all OFDM subcarriers capable of carrying. In the transmitter part of the system, it is assumed that these subcarriers are actively used to transmit data symbols modulated by either M-level quadrature amplitude modulation (M-QAM) or phase-shift keying (M-PSK). The frequency-domain complex-valued vector of data symbols, which is denoted by $X = [X[0], X[1], \cdots, X[N-1]]^T$, meets the Hermitian symmetry and the components in the subcarriers of the 0th (DC) and (N / 2) are set to zero as follows, [14].

$$X[k] = \begin{cases} 0, & \text{if } k = 0 \\ X^*[N-k], & \text{if } k = 1, 2, \cdots, (N/2) - 1 \\ 0, & \text{if } k = N/2 \end{cases} \tag{1}$$

Here, the complex conjugation denoted by $(*)$ operator. As a result, due to Hermitian symmetry, the time domain signal samples obtained at the output of

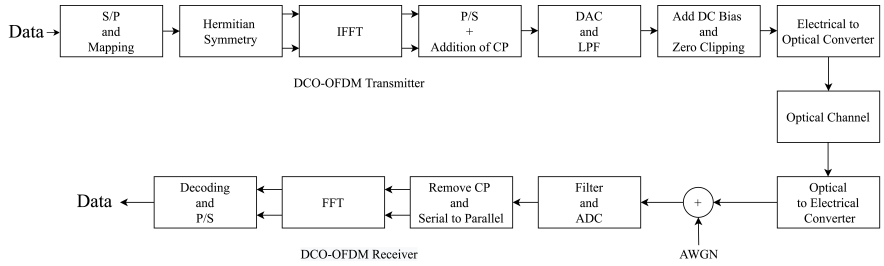

Fig. 1 DCO-OFDM Block Diagram

the inverse fast Fourier transform ($\mathcal{IFFT}$) become real valued [14]. The real, bipolar and antisymmetric time-domain signal vector $\mathbf{x} = [x[0], x[1], \cdots, x[N-1]]^T$ obtained at the end of these processes is denoted as follows:

$$x[n] = \sum_{k=1}^{N} X[k] e^{j2\pi kn/N} \tag{2}$$

In this equation, N is the number of points in $\mathcal{IFFT}$ and $X[k]$ is the kth component of $\mathbf{X}$. The number of data symbols carried by subcarriers in DCO-OFDM is $N/2 = 1$ due to Hermitian symmetry and the zero addition operation in $k = 0$ and $k = N/2$ subcarriers. A cyclic prefix (CP) of length Ncp is then added to the discrete-time samples. Here, the length of Ncp chosen is substantial, the length of Ncp must be greater than or equal to the maximum channel delay spread. It has been assumed as $Ncp \geq L$ in our computer simulations. After conversion from digital to analog, the electrical signal, $x(t)$, is generated in analog form. Note that due to the central limit theorem, $x(t)$ can be modeled approximately as a Gaussian process. It can clearly be said that its mean is zero and the variance can be determined by $\sigma_x^2 = E\{x^2(t)\}$. A proper DC bias is then added to $x(t)$ and the remaining residual negative peaks are clipped. As a result of these processes, a signal is obtained which is denoted by $x_{DCO}(t)$. Note that at this phase, a large DC bias will be required to eliminate the negative portion of $x(t)$ as the peak to average ratio of OFDM samples in the time domain is substantially high. However, adding a large DC bias increases optical energy per bit that is making the scheme highly inefficient in terms of optical power. Therefore, instead, a moderate DC bias is used in real applications, and then residual negative signal components are eliminated by clipping. This will, however, ultimately create a *clipping noise* and the BER performance of the scheme will be affected depending on the level of the clipping noise determined by the designer. The DC bias level, usually denoted by V_{DC}, is defined by the standard deviation $V_{DC} = \rho\sqrt{E\{x^2(t)\}}$, where ρ is constant and determined by $10\log(\rho^2+1)$ dB for a given distortion level in dB. As a result, time-domain samples obtained at the $\mathcal{IFFT}$ output of the DCO-OFDM system with a dc component are dented by $\tilde{x}[n] = x[n] + V_{\mathrm{DC}},\ n = 0, 1, \cdots, N-1$. Hence, after the clipping process, these samples become strictly positive valued as

$$x_c[n] = \begin{cases} \tilde{x}[n] \text{ if } \tilde{x}[n] \geq 0 \\ 0 \quad \text{ if } \tilde{x}[n] < 0 \end{cases} \tag{3}$$

In this equation, the clipping noise sample is represented by $e_c[n] = x_c[n] - \tilde{x}[n]$. Note that the amplitude of the DCO-OFDM time-domain samples that are not clipped for a large number of subcarriers can be approximated by a Gaussian distribution. So, the amplitude distribution of the clipped signal samples, which is denoted by $x_c[n]$, has a half-Gaussian distribution.

$$p_{x_c[n]}(x) = Q\left(V_{\mathrm{DC}}/\sigma_x\right)\delta(x) + \frac{u(x)}{2\pi\sqrt{\sigma_x}} e^{-(x-V_{\mathrm{DC}})^2/2\sigma_x^2}$$

In this equation, unit step function denoted by $u(.)$ and $Q(x) = (1/\sqrt{2})\int_x^\infty e^{-t^{2/2}}$. Then, the average transmitted electrical power $P_{\mathrm{elec;DCO}}$ of the above clipped signal is given by

$$\begin{aligned} P_{\mathrm{elec;DCO}} = E\{x_c^2\} &= \int_{-infty}^{\infty} x^2 p_{x_c}(x)dx \\ &= \left(\sigma_x^2 + V_{\mathrm{DC}}^2\right)\left(1 - Q(V_{\mathrm{DC}}/2\sigma_x)\right) \\ &\quad + \left(\sigma_x V_{\mathrm{DC}}/\sqrt{2\pi}\right)\exp\left(-V_{\mathrm{DC}}^2/2\sigma_x^2\right) \end{aligned} \tag{4}$$

Since $x_c[n] = \tilde{x}[n] + e_c[n]$, distorted data symbols caused by clipping noise in the frequency domain can be expressed as follows:

$$\begin{aligned} \mathbf{X_c} &= \mathcal{FFT}\{\mathbf{x_c}\} \\ &= \mathcal{FFT}\{\tilde{\mathbf{x}} + \mathbf{e_c}\} \\ &= \tilde{\mathbf{X}} + \mathbf{E_c} \end{aligned}$$

where, the clipping noise vector in the frequency domain is represented by $\mathbf{E_c} = [E_c[0], E_c[1], \cdots, E_c[N-1]]^T$. Through the Bussgang theorem [15], the OFDM signal received in the frequency domain can be expressed in matrix form as follows:

$$\mathbf{Y} = \mathbf{H}\tilde{\mathbf{X}} + \mathbf{C} + \mathbf{W} \tag{5}$$

where the optical channel coefficient matrix in the frequency domain is $\mathbf{H} = \mathrm{diag}[H_0, H_1, \cdots, H_{N-1}]$ and the N-dimensional dc-biased data vector represented by $\tilde{\mathbf{X}} = \mathbf{X} + \mathbf{u}$. Here, $\mathbf{u}$ is the FFT of the dc component and it expressed as $\mathbf{u} = [1, 0 \ \cdots, N-1]^T$. Finally, the clipping noise vector and the additive white Gaussian noise vector, whose each component has zero mean and variance σ_w^2, represented by $\mathbf{C} = \mathbf{H}\mathbf{E}_c$ and $\mathbf{W}$, respectively.

On the other hand, the channel impulse response (CIR) of the optical channel from source to destination link is sparse and characterized by

$$h(\tau) = \sum_{\ell=0}^{L-1} h_\ell \delta(\tau - \tau_\ell), \tag{6}$$

where L, h_ℓ and τ_ℓ denote the number of non-zero paths, the real-valued channel path amplitudes, and the path delays, respectively. The spareness of the visible light CIR comes from the fact that the electrical supply of the LEDs attached in series to a cable occurs with time delays. The components of the discrete frequency response of the sparse, multi-path VLC channel $\mathbf{H}$ can be expressed in terms of the CIR shown as:

$$H_k = \sum_{\ell=0}^{L-1} h_\ell \exp\left(-j\frac{2\pi k\tilde{\tau}_\ell}{N}\right),\ k = 0, 1, \cdots, N-1. \tag{7}$$

where $\tilde{\tau}_\ell = \tau_\ell/T_s$ is the ℓth normalized path delays with $T_s = T/N$ and T denotes the OFDM symbol duration. It is clear from (7) that $\mathbf{H} = \mathbf{Fh}$, where $\mathbf{F} = [\exp\left(-j\frac{2\pi k\tilde{\tau}_\ell}{N}\right)] \in \mathcal{C}^{N\times L}$ is the Fourier transform matrix and $\mathbf{h} = [h_1, h_2, \ldots, h_L]^T$.

3 Proposed Channel Estimation Technique

In this section, we propose an efficient sparse channel estimation technique for DCO-OFDM based VLC systems that also mitigate the inevitable effect of the clipping noise. In the light of the work, [16], an iterative channel estimation algorithm has been developed. In each iteration step of the algorithm, the estimation of the channel transfer function obtained in the previous estimation step is used to estimate the clipping noise samples. In the following subsection, we present an algorithm to estimate the initial the channel matrix $\mathbf{H}^{(0)}$ by means of the sparse channel path gains and the path delays, represented by $\mathbf{h} = [h_1, h_2, \ldots, h_L]^T$, and $\tau = [\tau_1, \tau_2, \ldots, \tau_L]^T$, in a pilot assisted and computationally efficient way. These parameters have been determined initially in [17] by the least-squares (LS) and the ESPRIT (Estimation of Signal Parameters via Rotational Invariant Techniques) algorithms. However, this technique requires estimation of the covariance matrix of the channel from the collected samples and several OFDM symbols need to be observed to approximate the covariance matrix. This would require more elaborate signal processing techniques such as the spatial smoothing, [19], increasing the computational complexity of the estimation algorithm considerably. As explained in the following subsection, the estimation problem is solved using one of the compress sensing techniques, called *ortogonal matching Pursuit (OMP)* [20], [18].

Subsequently, the iterative algorithm continues estimating $\mathbf{H}^{(i)}$ at each iteration step $i = 1, 2, \cdots$ until it converges to reach a minimum mean-squared error (MSE).

3.1 Estimation of Channel Path Delays and Path Gains

Through the equally spaced P pilot symbols, $X[i_p]$, each carried by the i_pth subcarrier for $p = 1, 2, \cdots, P$ the initial channel path gains and path delays

are estimated as follows: According to (5), the least square (LS) estimates of the channel frequency response at the pilot subcarriers of the OFDM symbol can be obtained as:

$$\hat{H}_{i_p,i_p} = \frac{Y[i_p]}{X[i_p]} = H_{i_p,i_p} + Z[i_p] \tag{8}$$

where $Z[i_p] = (C[i_p] + W[i_p])/X[i_p]$, $p = 1, 2, \cdots, P$. From (6) and (7), (8) can be expressed in vector form

$$\hat{\mathbf{H}}_P = \mathbf{A}\mathbf{h} + \mathbf{Z}_P \tag{9}$$

where $\hat{\mathbf{H}}_P = [\hat{H}_{i_1,i_1}, \cdots, \hat{H}_{i_P,i_P}]^T$, $\mathbf{Z}_P = [Z_{i_1}, \cdots, Z_{i_P}]^T$ and $\mathbf{A}$ is a $P \times L$ matrix whose (m, ℓ)'th element is $\mathbf{A}[m, \ell] = e^{-j2\pi i_m \tau_\ell / N}$.

To solve the sparse estimation problem with the observation model in (9), we focus on a conventional OMP algorithm that iteratively estimates one path delay τ_ℓ at a time and solves a constained LS problem at each iteration to measure the fitting error [18]. However, in practice, the sparsity assumption does not always hold and consequently may not represent a truly sparse channel impulse response due to the non-integer normalized path delays in the equivalent discrete-time baseband representation of the channel. Therefore, such an estimated channel may differ substantially from the original channel. The A/D conversion at the input of the OFDM receiver is implemented first with an oversampling rate $R_s^{(\varrho)} = \varrho/T_s, \varrho = 1, 2, \cdots$, leading to a finer delay resolution matrix $\mathbf{A}_P^{(\varrho)} \in \mathcal{C}^{P \times N_\tau}$, called a *dictionary matrix*. The columns of $\mathbf{A}_P^{(\varrho)}$ correspond to the $\mathcal{T}_\ell^{th}$ discrete multipath channel tap delays, where ϱ is the oversampling factor, and $1/T_s$ is the baseband Nyquist sampling rate. Consequently, the real-valued normalized path delays $\widetilde{\tau}_\ell, \ell = 0, 1, \cdots, L-1$ can be discretized as $\mathcal{T}_\ell = \lfloor \varrho \widetilde{\tau}_\ell \rfloor$ and take values from the set of the possible discrete path delays

$$\mathcal{T}_\ell \in \{0, 1, 2, \cdots, N_\tau - 1\}, \tag{10}$$

where $N_\tau = \varrho L_{CP}$, $L_{CP} = T_{CP}/T_s$. Given $\mathcal{T}_\ell$ in (10), $\mathbf{A}_P^{(\varrho)}$ can be written as

$$\mathbf{A}_P^{(\varrho)} = \begin{bmatrix} e^{-j2\pi p_1 0/(N\varrho)} & \cdots & e^{-j2\pi p_1 (N_\tau - 1)/(N\varrho)} \\ e^{-j2\pi p_2 0/(N\varrho)} & \cdots & e^{-j2\pi p_2 (N_\tau - 1)/(N\varrho)} \\ . & \cdots & . \\ . & \cdots & . \\ e^{-j2\pi p_P 0/(N\varrho)} & \cdots & e^{-j2\pi p_P (N_\tau - 1)/(N\varrho)} \end{bmatrix}. \tag{11}$$

Based on the associated discrete random channel tap positions $\{\mathcal{T}_\ell\}_{\ell=0}^{L-1}$, the received signal in (9) can be rewritten as

$$\hat{\mathbf{H}}_p = \sum_{\ell=0}^{L-1} \mathbf{a}_{r_\ell} h_\ell + \mathbf{V}_P \ , \tag{12}$$

where $\mathbf{a}_{r_\ell}$ is the r_ℓ^{th} column vector of the finer resolution matrix $\mathbf{A}_P^{(\varrho)}$ whose columns correspond to the $(\mathcal{T}_\ell)^{th}$ channel tap delays. For a given $r_\ell \Leftrightarrow (\mathcal{T}_\ell)$, the k^{th} component of $\mathbf{a}_{r_\ell}$ is determined from $\mathbf{A}_P$ in (11) as

$$a_{r_\ell}[k] = A_P[k,\ell]\Big|_{\widetilde{\tau}_\ell = \mathcal{T}_\ell/\varrho}. \tag{13}$$

Note that for $\mathcal{T}_\ell \in \{0,1,\cdots N_\tau - 1\}$, total number of columns of $\mathbf{A}_P^{(\varrho)}$ is N_τ and they are labelled as $r_\ell = 1,2,\cdots,N_\tau$. The conversion between r_ℓ and $(\mathcal{T}_\ell)$ can be easily obtained as:

$$r_\ell = \mathcal{T}_\ell + 1, \text{ with, } \mathcal{T}_\ell = \lfloor r_\ell \rfloor - 1.$$

To estimate the discretized channel path delay $r_\ell \Leftrightarrow (\mathcal{T}_\ell)$ from the observation vector in (12), we employ the OMP algorithms that involves iteratively estimates one r_ℓ at a time and solves a constraint least-square (LS) problem at each iteration step to determine the fitting error, as mentioned above. Once the delays $\{\tau_\ell\}$ are estimated, the LS estimate of the channel path gains vector $\mathbf{H}$ is obtained as,

$$\widehat{\mathbf{h}} = \left(\widehat{\mathbf{A}}^\dagger \widehat{\mathbf{A}}\right)^{-1} \widehat{\mathbf{A}}^\dagger \widehat{\mathbf{H}}_p. \tag{14}$$

where $\widehat{\mathbf{A}}$ is the estimate of $\mathbf{A}$ with, for $m = 0,\cdots,N-1;\ \ell = 0,\cdots,L-1$, $\widehat{\mathbf{A}}[m,\ell] = e^{-j2\pi i_m \widehat{\tau}_\ell/N}$.

3.2 Iterative Channel Estimation Algorithm

In this subsection, we introduce the iterative channel estimation algorithm that relies on the estimation of clipping noise at each iteration and compensating for the effect on the observed signal at the output of the $\mathcal{FFT}$ process at the receiver. As explained in the previous section, the initial channel estimation $\mathbf{H}^{(0)}$ is defined as $\mathbf{H}^{(0)} = \mathbf{F}_L \widehat{\mathbf{h}}$, and it is determined from the estimated channel impulse response by pilot symbols. Here, $\mathbf{F}_L$ is an $N \times L$ DFT matrix. Following this step, data symbols are detected from (5) as given below:

$$\mathbf{X}^{(0)} = \mathcal{DETECT}\left\{ \left(\mathbf{H}^{(0)}\right)^{-1} \mathbf{Y} \right\} \tag{15}$$

from which the initial estimates of the transmitted OFDM time-domain samples are obtained by the $\mathcal{IFFF}$ operation as

$$\mathbf{x}^{(0)} = \mathcal{IFFT}\{\mathbf{X}^{(0)}\}$$

where a *hard decison* process is denoted with $\mathcal{DETECT}\{a\}$ operator. In the following iteration step, an estimate of clipping noise is obtained as follows:

$$\mathbf{E}_c^{(0)} = \mathcal{FFT}\left\{ \mathbf{x_c}^{(0)} - \tilde{\mathbf{x}}^{(0)} \right\}.$$

Here, if $\mathbf{X}^{(1)} \approx \mathbf{X}$, i.e. BER is small enough, then $\mathbf{E}_c^{(0)} \approx \mathbf{E}_c$. Under this condition, the channel and clipping noise estimates obtained in the previous iteration can be used to easily obtain the next estimated values as shown in Algorithm 1.

Algorithm 1 Estimation of sparse VLC Channel in the Presence of Clipping Noise

Input: Observation vector: $\mathbf{Y}$, initial estimates: $\mathbf{H}(0)$, $\mathbf{E}_c^{(0)}$
Output: Final estimated channel matrix $\mathbf{H}^{(N_{iter})}$
for $i = 1$ to N_{iter} **do**

$$\mathbf{Y} \Longrightarrow \mathbf{Y} - \mathbf{H}^{(i-1)}\mathbf{E}_c^{(i-1)} \tag{16}$$

$$\mathcal{H} \equiv \left(\mathbf{X}^{(i-1)}\right)^{-1}\mathbf{Y} \tag{17}$$

$$\mathbf{h}^{(i)} = \left(\widehat{\mathbf{A}}^{\dagger}\widehat{\mathbf{A}}\right)^{-1}\widehat{\mathbf{A}}^{\dagger}\mathcal{H} \tag{18}$$

$$\mathbf{H}^{(i)} = \mathbf{F}_L\mathbf{h}^{(i)} \tag{19}$$

$$\mathbf{X}^{(i)} = \mathcal{DETECT}\left\{\left(\mathbf{H}^{(i)}\right)^{-1}\mathbf{Y}\right\} \tag{20}$$

$$\mathbf{x}^{(i)} = \mathcal{IFFT}\{\mathbf{X}^{(i)}\} \tag{21}$$

$$\mathbf{E}_c^{(i)} = \mathcal{FFT}\left\{\mathbf{x_c}^{(i)} - \tilde{\mathbf{x}}^{(i)}\right\} \tag{22}$$

end for

4 Simulation Results

In this section, we present computer simulation results to investigate the MSE and BER performance of the iterative channel estimation algorithm proposed for DCO-OFDM systems in the presence of clipping noise. In addition, the effects of different pilot spacings, as well as modulation types on the initial BER vs. SNR performance, were taken into account and studied. The channel model considered in the simulations is assumed to be formed as four LEDs, placed at the corners of a square with a certain edge length on the ceiling of a closed environment and a receiving photodiode placed at the base of the environment (Figure 2). As shown in Figure 3.(a), the impulse response of the optical channel occurs in a sparse and frequency-selective structure, as the electrical supply of the LEDs connected in series with a cable causes a certain time delay. The system parameters for the simulation scenario are given in Table I. In the computer simulations, it is assumed that D/A converter and photodetector are ideal so that optical-to-electrical conversion constant ξ and electrical-to-optical conversion constant R are chosen as $\xi = R = 1$. Also we adopt using the transmitter transmit signal energy, $E_{b_{\text{elec;DCO}}}$ per additive

Gaussian noise energy spectral density N_0 as a signal-to-noise ration metric defined as

$$\frac{E_{b_{\text{elec;DCO}}}}{N_0} = \frac{E\{x_c^2\}}{R_{\text{b,DCO}} N_0}.$$

We first investigate the MSE and BER performance of the initial channel estimation algorithm, since the quality of the initial channel estimation affects the convergency of the iterative algorithm to a true solution point as well as the final MSE and BER performances. In Figure 4, the BER vs. SNR curves are shown for the initial channel estimate $\mathbf{H}^{(0)}$ with BPSK, QPSK, and 16-QAM modulations with pilot spacing $\Delta_p = K/P = 4$ and the clipping noise level is set to $B = 2$ dB. From these curves, it is seen that while BPSK and QPSK modulations yield sufficiently good BER performances to feed in the subsequent iterations. However, for 16-QAM, smaller pilot spacings should be chosen such as $\Delta_p = 3$ or even to $\Delta_p = 2$ for the iterative algorithm to reach its ultimate BER performance in a given number of iterations.

Table 1 Simulation Parameters

Number of subcarriers, N	256
Bandwidth, BW	2 MHz
Sampling frequency, fs	1Ghz
Pilot symbols frequency	1/4
Multipath channel gains [dB]	[S1, S2, S3, S4] [1.2*1e-04 0.65*1e-04 1*1e-04 1.8*1e-04]
Modulation	BPSK, QPSK, 16-QAM
Max iteration step, imax	3
Pilot spacings, Δ_p	2,3,4

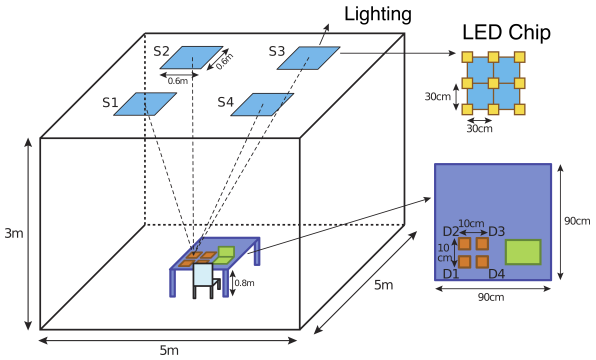

Fig. 2 VLC channel model simulation environment

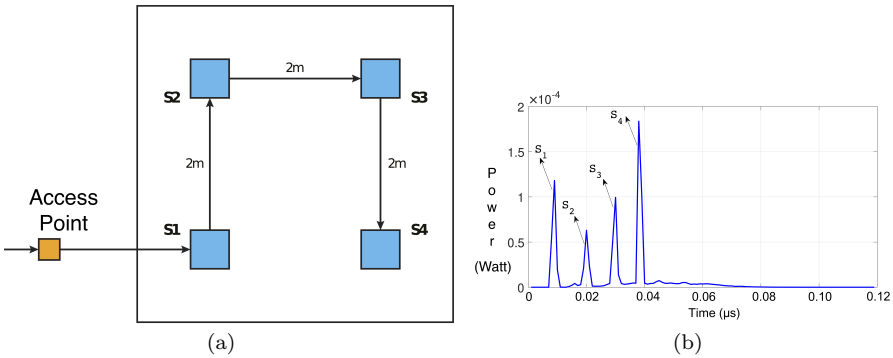

Fig. 3 (a) Realistic cabling topology (CAT-5). (b) Channel impulse response due to delay in cabling

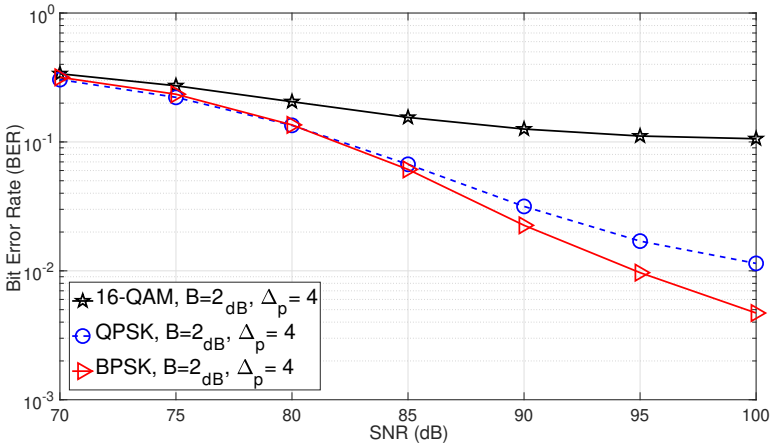

Fig. 4 Initial BER vs. SNR performances for BPSK, QPSK, 16-QAM

On the other hand, to choose good initial values for the unknown channel parameters and to ensure a fast start-up in the equalization/detection operation following the channel estimation process, the selection of the number of pilots symbols P known by the receiver is important. Note that $P \geq L_{CP}$ to identify the channel, where L_{CP} is the number of OFDM prefix symbols. When the number of subcarriers, K, is large, however, this does not create a significant degradation in spectrum efficiency since L_{CP} takes small values with respect to the total number of subcarriers carrying the data. To interpolate the channel estimates, initially, there exists a minimum subcarrier spacing $\Delta_{p,\min} < 1/2\tau_{\max}$, where $\tau_{\max}$ is the maximum delay spread of the channel. Based on this fact, from the system parameters, given by Table I, and $\tau_{\max} = 0.04$ μsec, (as seen from Figure 3.(b)), the minimum number of OFDM subcarriers comes out to be $\Delta_{p,\min} \leq 3.5$. In Figure 5, the effect of pilot spacings is investigated for $\Delta_p = 2, 3, 4$ on the initial MSE and SER

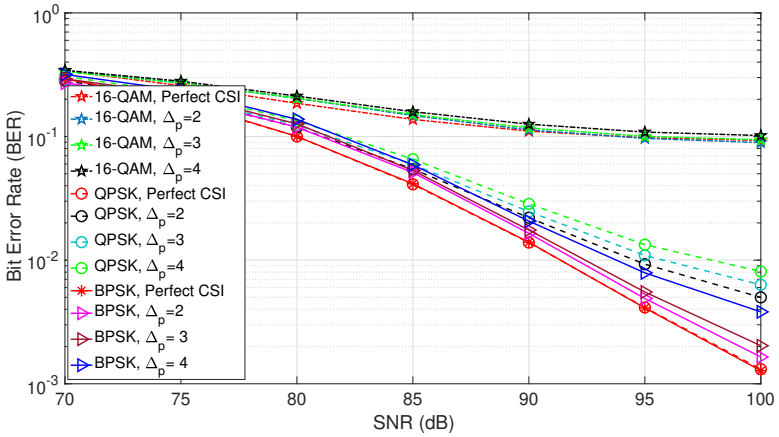

Fig. 5 Effect of pilot spacings on the BER performance for BPSK, QPSK and 16-QAM signaling

performance at different SNR values using BPSK, QPSK and 16QAM modulation. It can be seen from these curves that the initial channel estimation algorithm can tolerate for a pilot spacing of $\Delta_p = 3$. However, the BER and MSE performance degrade as the pilot spacing increases beyond that. It is also concluded from Figure 5 that the BER performance converges to that of the perfect CSI performance in a maximum of two iterations for both BPSK and QPSK signaling schemes. In Figures 6 and 7, the MSE and BER performance curves of the channel estimation algorithm for QPSK modulation are obtained on the subsequent iteration steps for $B = 2$ dB and $B = 1$ dB levels of clipping noise. From these curves, it is concluded that the proposed iterative algorithm contributes substantially to both MSE and BER performances of the system. In addition, it is observed that almost all of these contributions and gains are obtained during the 1st iteration; as a small increase is observed in the BER performance, the improvement in the MSE performance becomes small enough to be neglected in the second iteration. Therefore, we conclude from these graphs that the nonlinear disturbance effects caused by clipping noise are greatly reduced by the proposed algorithm in a maximum of two iteration steps. However, it can be seen that the obtained BER performance curve does not converge to the BER curve when the channel is fully known, and also that the MSE performance does not converge to the MSE curve when all data symbols transmitted when the channel is perfectly known. This is mainly because the time-domain samples at the OFDM output in the transmitter are clipped as a result of a nonlinear process.

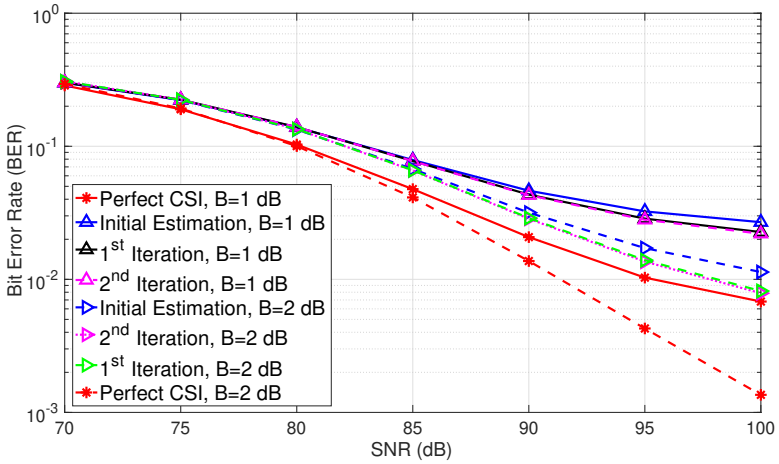

Fig. 6 BER vs. SNR curves for B=1dB and B=2dB

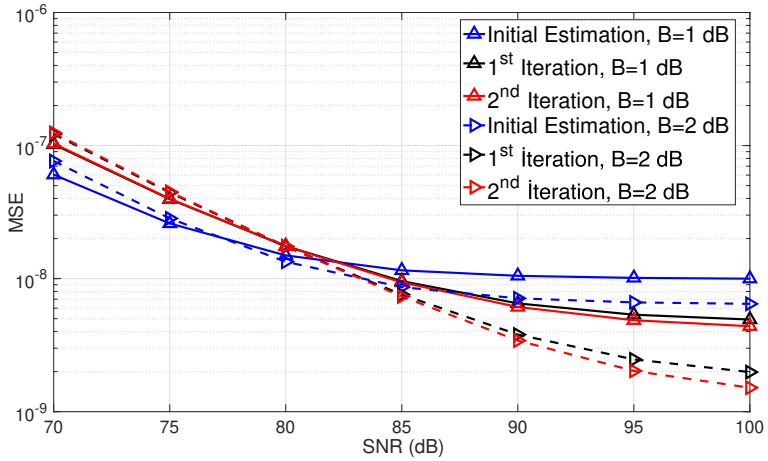

Fig. 7 MSE curves for B=1dB and B=2dB

5 Conclusions

A new and novel iterative channel estimation algorithm was proposed for the estimation of sparsely modeled indoor VLC channels under the effect of clipping noise. Both the MSE performance of this algorithm and the system BER performance in transmissions performed with a VLC system using the DCO-OFDM technique has been examined by computer simulations. The initial channel parameters are estimated by the pilot aided OPM algorithm. Then, in each iteration step, the clipping noise was estimated by using the previous channel values and the effect was compensated in the frequency-domain. It

has been shown by computer simulations that the algorithm was very effective in minimizing the effects of inevitable clipping noise, especially affecting these systems. In particular, the MSE and BER performance of the system for different clipping noise levels for DCO-OFDM systems over sparse VLC channels was investigated, and it was found that the algorithm reached the maximum performance of the system in two iterations, at most. It was also concluded that the system had better BER performance for small SNR values at low clipping noise levels, but larger SNR values showed significantly better BER performance for larger SNR values.

6 Declarations

6.1 Funding

This work was supported by the Scientific and Technical Research Council of Turkey (TUBITAK) under the 1003-Priority Areas R&D Projects support Program No:218E034.

6.2 Conflicts of interest/Competing interests

'Not applicable'

6.3 Availability of data and material (data transparency)

'Not applicable'

6.4 Code availability (software application or custom code)

'Not applicable'

6.5 Authors' contributions

'Not applicable'

References

1. D. J. T. Heatley, D. R. Wisely, I. Neild, and P. Cochrane, "Optical wireless: the story so far," *IEEE Commun. Mag.*, vol. 36, no. 12, pp. 72–74, 79–82, 1998.
2. Jean Armstrong, "OFDM for Optical Communications," *J. Lightwave Technol.*, no.27, pp. 189-204, 2009.
3. S. Dissanayake and J. Armstrong, "Comparison of ACO-OFDM, DCO- OFDM and ADO-OFDM in IM/DD systems," *J. Lightwave Technol.*, vol. 31, no. 7, pp. 1063–1072, Apr. 2013.

4. S. Dimitrov, S. Sinanovic and H.Haas,"Clipping Noise in OFDM-Based Optical Wireless Communication Systems," *IEEE Trans. Commun.*, vol. 60, no. 4, pp. 1072-1081, April 2012.
5. H. Dogan, O. Saylı, E. Panayirci, "Pilot assisted channel estimation for asymmetrically clipped optical OFDM over visible light channels", *2016 IEEE Int. Black Sea Conf. on Communications and Networking (BlackSeaCom)*, 6-9 June 2016, Varna, Bulgaria.
6. O. Sayli, H. Dogan, E. Panayirci, "On channel estimation in DC Biased optical OFDM systems over VLC channels", *2016 Int. Conf. on Advanced Technologies for Communications (ATC)*, 12-14 Oct 2016, Hanoi, Vietnam.
7. J. C. Estrada-Jiménez, B. G. Guzmán, M. J. Fernández-Getino García and V. P. G. Jiménez, "Superimposed Training-Based Channel Estimation for MISO Optical-OFDM VLC," in *IEEE Transactions on Vehicular Technology*, vol. 68, no. 6, pp. 6161-6166, June 2019, doi: 10.1109/TVT.2019.2909428.
8. B. Lin, Z. Ghassemlooy, J. Xu, Q. Lai, X. Shen and X. Tang, "Experimental Demonstration of Compressive Sensing-Based Channel Estimation for MIMO-OFDM VLC," in *IEEE Wireless Communications Letters*, vol. 9, no. 7, pp. 1027-1030, July 2020, doi: 10.1109/LWC.2020.2979177.
9. Jie Du, Honggui Deng, Xuewen Qian, and Chaoyang Zhang "Channel estimation scheme based on compressed sensing and parameter estimation for an orthogonal frequency division multiplexing visible light communications system," *Optical Engineering* 55(11), 116109 (22 November 2016).
10. Alamir, A., Esmaiel, H. & Hussein, H.S. Efficient Optical MIMO–OFDM Channel Estimation Based on Correntropy Compressive Sensing. *Wireless Pers Commun.* 115, 1955–1971 (2020).
11. L. Wu, J. Cheng, Z. Zhang, J. Dang and H. Liu, "Channel Estimation for Optical-OFDM-Based Multiuser MISO Visible Light Communication," in *IEEE Photonics Technology Letters*, vol. 29, no. 20, pp. 1727-1730, 15 Oct.15, 2017, doi: 10.1109/LPT.2017.2747147.
12. X. Chen and M. Jiang, "Adaptive Statistical Bayesian MMSE Channel Estimation for Visible Light Communication," in *IEEE Trans. on Signal Processing*, vol. 65, no. 5, pp. 1287-1299, 1 March1, 2017, doi: 10.1109/TSP.2016.2630036.
13. Xi Wu, Zhitong Huang, Yuefeng Ji, "Deep neural network method for channel estimation in visible light communication," *Optics Communications*, Volume 462, 2020. (2002)
14. S. Dissanayake and J. Armstrong, "Comparison of ACO-OFDM, DCO-OFDM and ADO-OFDM in IM/DD systems," *J. Lightwave Technol.*, vol. 31, no. 7, pp. 1063–1072, (Apr. 2013)
15. J. J. Bussgang. "Crosscorrelation functions of amplitude-distorted Gaussian signals", *Tech. Rep. 216*, Department of Computer Science, Michigan State University, (March 1952)
16. S. C. Schwartz, J. Zhang and D. Gu, "Iterative channel estimation for OFDM with clipping," *The 5th Int. Symp. Wireless Personal Multimedia Communications*, pp. 1304-1308 vol.3, Honolulu, HI, USA.
17. E. B. Bektas and E. Panayirci, "Sparse Channel Estimation with Clipping Noise in DCO-OFDM Based VLC Systems," *2020 IEEE Int. Black Sea Conf. on Communications and Networking (BlackSeaCom)*, Odessa, Ukraine, 2020, pp. 1-5, doi: 10.1109 BlackSeaCom48709.2020.9235008.
18. J. A. Tropp and A. C. Gilbert, "Signal recovery from random measurements via orthogonal matching pursuit," *IEEE Trans. Inf. Theory*, vol. 53, no. 12, pp. 4655-4666, Dec. 2007.
19. T.-J. Shan, M. Wax, and T. Kailath, "On spatial smoothing for direction- of-arrival estimation of coherent signals," *IEEE Trans. Signal Process.*, vol. 33, no. 4, pp. 806–811, Aug. 1985.
20. D. Donoho, "Compressed sensing," *IEEE Trans. Inf. Theory*, vol. 52, no. 4, pp. 1289–1306, Apr. 2006.

Ekin Basak Bektas received the B.Sc. and M.Sc. degrees in electronics engineering from Kadir Has University, Istanbul, Turkey, in 2018 and 2020, respectively. Her research interests include signal processing, channel estimation, and optical wireless communications.

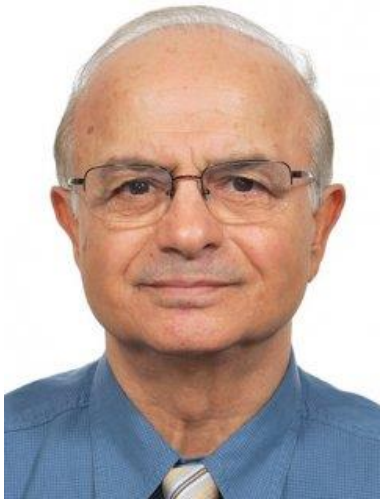

Erdal Panayirci received the Diploma Engineering degree in electrical engineering from Istanbul Technical University, Istanbul, Turkey, and the Ph.D. degree in electrical engineering and system science from Michigan State University, USA. Until 1998 he has been with the Faculty of Electrical Engineering, Istanbul Technical University, where he was a Professor and the Head of the Telecommunications Chair. He is currently a Professor of Electrical Engineering and the Head of the Electrical and Electronics Engineering Department with Kadir Has University, Istanbul. He has been the Principal Coordinator of a 6th and 7th Frame European Project called the Network of Excellent on Wireless Communications and WIMAGIC Strep Project for two years, representing Kadir Has University. He has authored extensively in leading scientific journals and international conference and co- authored the book Principles of Integrated Maritime Surveillance Systems (Boston, Kluwer Academic Publishers, 2000). His recent research interests include communication theory, advanced signal processing techniques and their applications to wireless electrical, underwater, and optical communications. He was an Editor of the IEEE Transactions on Communications in the areas of synchronizations and equalizations from 1995 to 2000. He served as a member of IEEE Fellow Committee from 2005 to 2008. He was the Technical Program Co-Chair of the IEEE International Conference on Communications and the Technical Program Chair of the IEEE PIMRC held in Istanbul, in 2006 and 2010, respectively. He was the Executive Vice-Chairman of the upcoming IEEE Wireless Communications and Networking Conference held in Istanbul in 2014. He is currently a member of the IEEE GLOBECOM/ICC Management and Strategy Standing Committee and the Head of the Turkish Scientific Commission on Signals and Systems of International Union of Radio Science. He is an IEEE Life Fellow.

Supplementary Files

This is a list of supplementary files associated with this preprint. Click to download.

- file.ds_store
- history.txt
- readme.txt